

Inventory of Rock Slope Deformations Affecting Folded Sedimentary Layers in Moderate Relief Context: The Case of the Livingstone Range Anticlinorium, AB, Canada

F. Humair, J.-L. Epard, M.-H. Derron, M. Jaboyedoff, D. Pana, C. Froese, and A. Pedrazzini

Abstract

This contribution investigates the distribution of rock slope deformations (RSD) and their relationships with tectonic structures, lithological and topographic contexts. This is performed in a moderate relief context (1,100–2,500 masl.) affected by thin-skin tectonic. The proposed inventory, along the *Livingstone range anticlinorium* (LRA), contains 160 gravitational events that are spatially clustered in four areas. The thrust-folds properties (density, geometry and lithology) and the local relief appear to primary influence the development of RSD in this context.

Keywords

Thin skin tectonic • Sedimentary layers • Rock slope deformations • Inventory

99.1 Objectives and Context

Different predisposing (structural settings, rock mass quality characteristics, lithology, slope geometry, groundwater...), preparatory (glaciation/deglaciation, uplift rate and differential uplift, local relief, modification of the slope geometry...) and triggering (seismic shaking, climate...) factors are frequently associated with the spatial and temporal evolution of rock slope deformations (RSD) in different mountain belts (Schmidt and Montgomery 1995; Hermanns et al. 2001; Agliardi et al. 2009; Antinao and Gosse 2009; Clarke and Burbank 2010; Crosta et al. 2013). However, most of the studies focus in high relief mountain ranges and the development of RSD in fold and thrust belts in moderate relief topography is still poorly documented. The purpose of this

contribution is to propose an inventory of RSD types in such a context in order to investigate the spatial relationships between this process and the structural / lithological characteristics. Our investigations are carried out along the *Livingstone Range anticlinorium* (LRA), in southwestern Alberta, Canada. This 80 km long slightly arcuate mountain range constitutes the easternmost part of the Canadian Rocky Mountain fold-and-thrust belt, and consists of flexural-slip thrust propagation folds affecting Devonian to Jurassic carbonates and clastic rocks (Cooley et al. 2011; McMehan and Stockmal 2013).

99.2 Methods and Approach

RSD are mapped and documented at the scale of the entire LRA ($\sim 1,490 \text{ km}^2$) using High Resolution Digital Elevation Model (cell size 1 m) and Google Earth™. As proposed by Pedrazzini et al. (submitted), the RSD have been classified based on a simplification of Hutchinson (1998): rockslide and rock-avalanche (RRA), roto-translational slides (RTS) and deep-seated gravitational slope deformations (DSGSD). The spatial relationship between RSD has been estimated using a derivative of the Ripley's K-function (Ripley 1977), namely the L-function (Besag 1977) to test whether the events are clustered or randomly distributed (Tonini et al. 2013, Pedrazzini et al. submitted). Plotted against the search radius (r),

F. Humair (✉) · J.-L. Epard · M.-H. Derron · M. Jaboyedoff
ISTE, University of Lausanne, Lausanne, Switzerland
e-mail: florian.humair@unil.ch

D. Pana
Alberta Geological Survey, Edmonton, Canada

C. Froese
Alberta Energy Regulator, Calgary, Canada

A. Pedrazzini
Office de l'environnement, St-Ursanne, Canton du Jura,
Switzerland

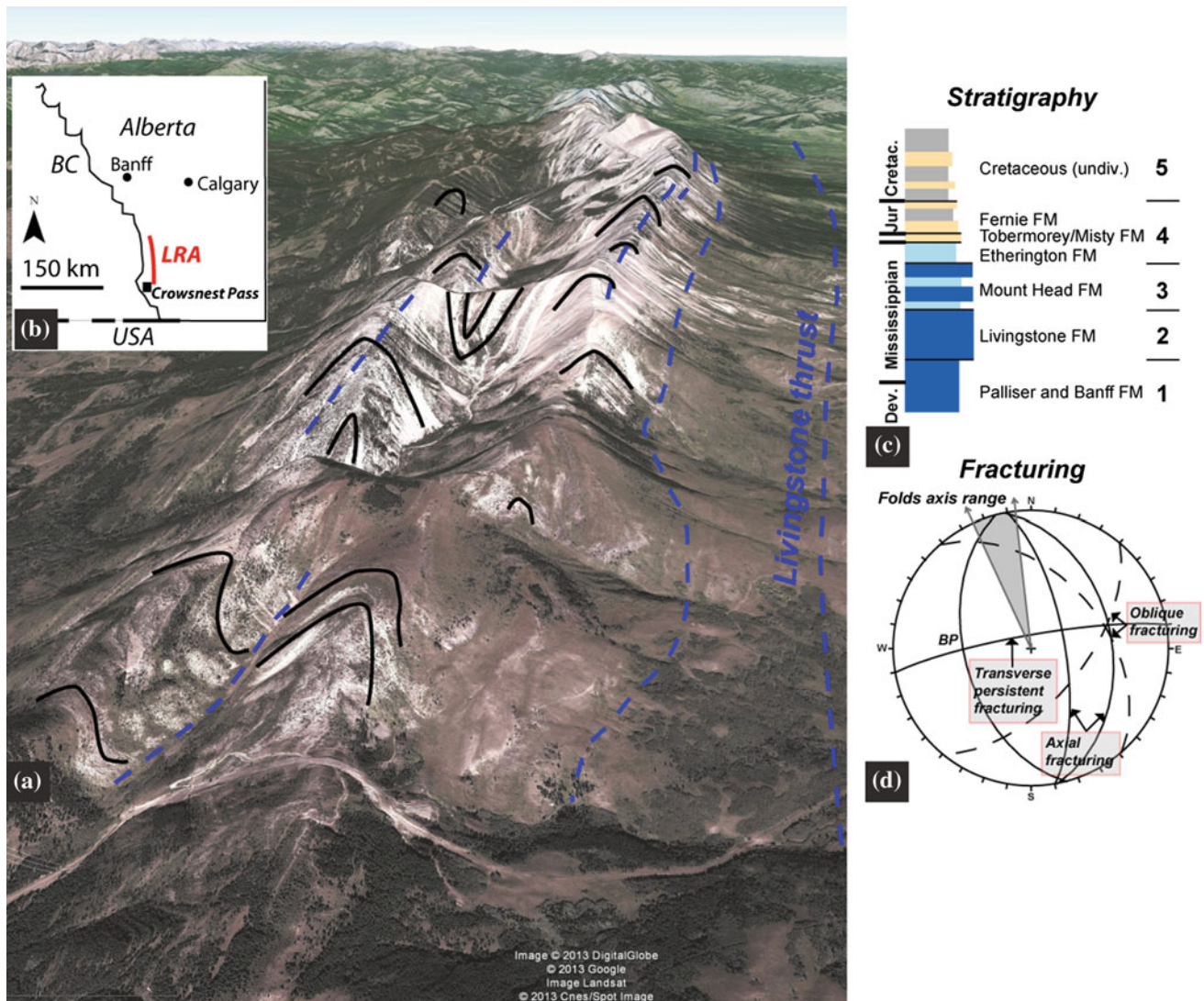


Fig. 99.1 **a** Northward Google Earth™ view of the southern part of the LRA (bedding in *black* and thrusts in *blue*). **b** Location of the study area. **c** Simplified stratigraphic log with the five lithological groups

attributed in the present study (limestone, dolostone, sandstone, shale). **d** Simplified fracturing pattern affecting the LRA summarized in five joint sets plus the bedding (plotted for the western fold limbs)

$L(r)$ displays a value of zero for randomness, positive and negative values for respectively clustered or dispersed data structure. The maximal value was then used as research radius to map the spatial density of the detected RSD. This step was performed using a Kernel density function (Silverman 1986) in a GIS environment. The local relief has been calculated by subtracting the minimum elevation within a circular window of 3 km radius from the maximum elevation. Compared to other studies (Khueni and Pfiffner 2001; Montgomery and Brandon 2002; Pedrazzini et al. submitted), a smaller radius is selected as the width of this particular valley is significantly smaller than in higher mountain belts.

In addition, the influence of the regional scale structural setting was investigated considering two parameters: the distance of the RSD events to the anticline axial traces and faults (euclidian distance) and the topographic / bedding-plane intersection angle (TOBIA) as proposed by Meentemeyer and Moody (2000). The TOBIA model discriminates the slopes in three classes: anacinal (bedding dips in the direction opposite to the slope), cataclinal (bedding dips in the same direction) and orthoclinal (dip direction of the bedding perpendicular to the dip direction of the slope). Ordinary kriging was used to interpolate dip and dip direction from the punctual information (2,676 data).

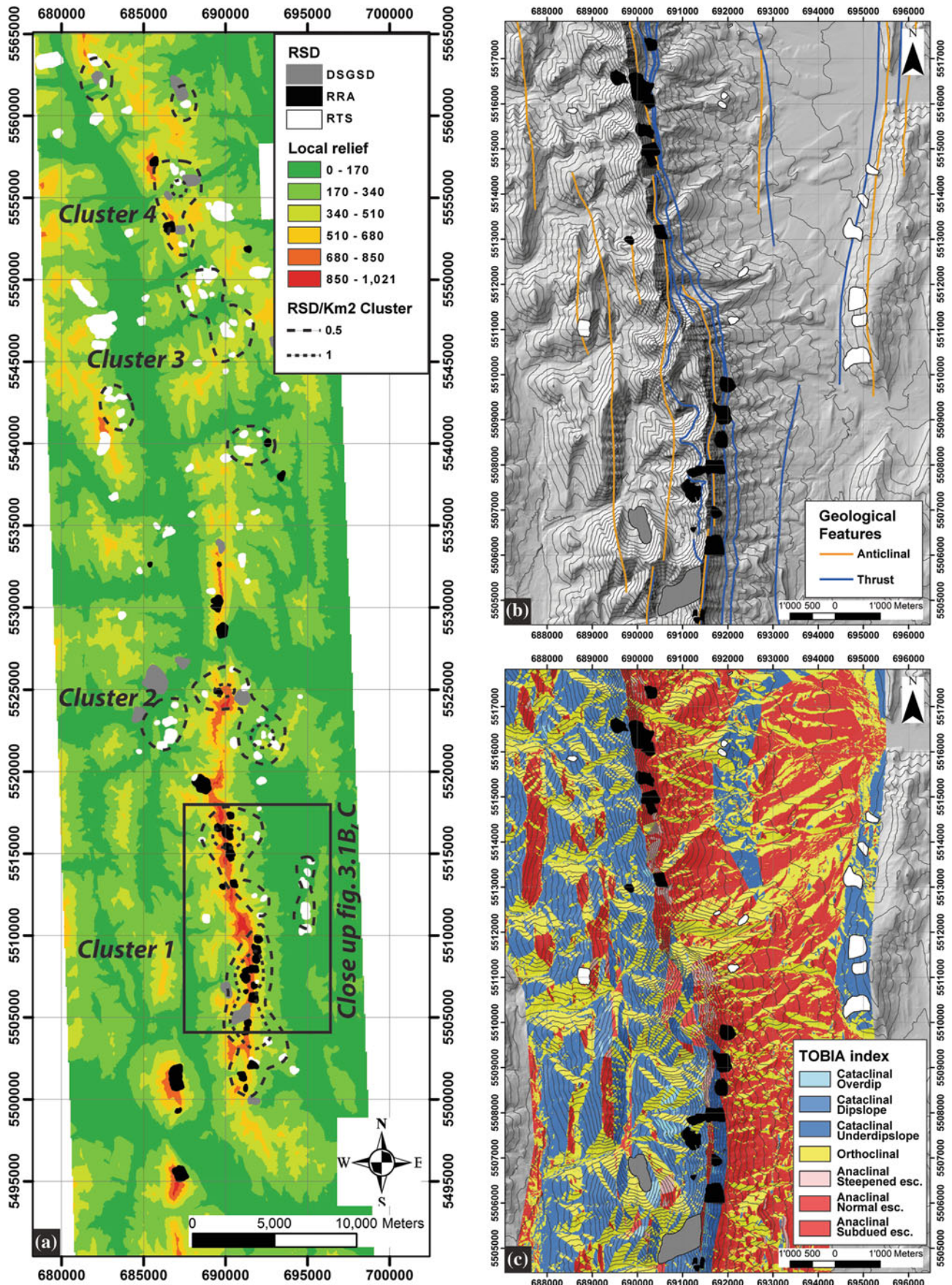


Fig. 99.2 a LRA RSD inventory distribution displayed on the local relief map obtained by the HRDEM (cell size 10 m). The kernel density contours of 0.5 and 1 RSD/km² calculated for the whole RSD dataset are shown. **b** and **c** Close up on the main RSD cluster (cluster 1).

b Tectonic map (anticlines, main thrusts). **c** Detailed TOBIA model classification dividing the slope-bedding intersection in seven different classes (see Meentemeyer and Moody 2000 for more details)

99.3 Rock Slope Deformations Inventory Along the LRA

The rock slope deformations (RSD) database comprises 160 events: 44 RRA, 101 RTS and 15 DSGSD. The spatial distribution of the RSD categories under study shows that they are spatially clustered in a range of 0 to 6 km with a maximal value at approximately 2,050 m, aside from the DSGSD's event that are comprised within the error envelope (Fig. 99.3b). The number of events inside a circle of about 2 km is therefore higher than expected for a random distribution process. Figure 99.2 shows the spatial distribution of the RSD by categories and the contours of the RSD density (0.5 and 1 RSD/km²), highlighting 4 main zones of clustering. RRA are almost all (69 %) distributed in the south of the LRA (cluster 1), whereas RTS are located from the middle to the northern part (clusters 2 and 3). Cluster 4 contains all types of RSD. The local relief map (Fig. 99.2a)

highlights that the relief is higher around cluster zones 1 and 4 compared to the whole study area, reflecting an association between RRA and local relief. Less influence of local relief on RTS and DSGSD is observed as their values are in the range of the study area (Fig. 99.3c). A comparison between the lithologies affected by the failure surfaces and the categories of RSD reveals that 85 % of the RRA failure surfaces are concentrated in competent carbonate lithologies (stratified and massive limestone and dolostone) whereas more than 95 % of the RTS are linked with less competent interlayered clastic lithologies comprising shale, sandstone and thin bedded dolostone (Fig. 99.3d). On the other side, DSGSD affect all lithological groups. Even if a general trend emerges, a clear linkage cannot be assessed since the lithological repartition among the study area has not been performed. Nonetheless, the investigations of the main structural settings' influence show that 28 % of the RSD intersect an anticline axial trace and 53 % are located within

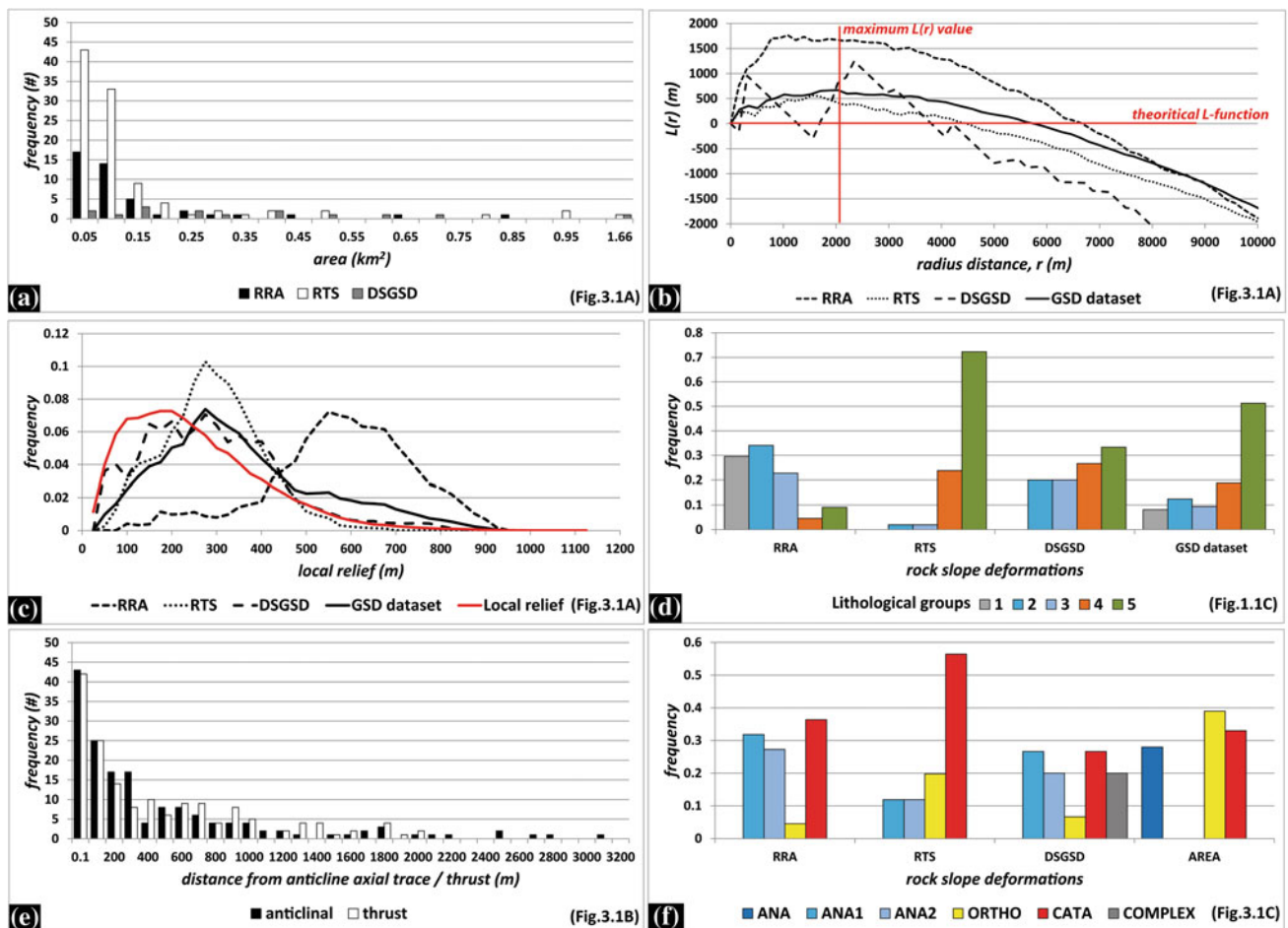


Fig. 99.3 Analysis of RSD inventory. **a** RSD frequency-area distribution. **b** Ripley's L-function for the GSD. *Horizontal red line* represents the theoretical L-function and *vertical red line* corresponds to the L(r) maximum value (i.e. the optimal distance of clustering) which is used as the search radius for the Kernel density calculation (Fig. 99.2a). **c** Comparison between local relief distribution in the entire

study area and the distribution within the RSD areas. **d** RSD frequency-lithological groups (Fig. 99.1c). **e** RSD frequency—distance to anticline/thrusts. **f** RSD frequency—attitude of the bedding (TOBIA model). ANA = anaclinal, ANA1 and ANA2 = anaclinal subgroup 1 and 2, ORTHO = orthoclinal, CATA = cataclinal, COMPLEX = complex RSD

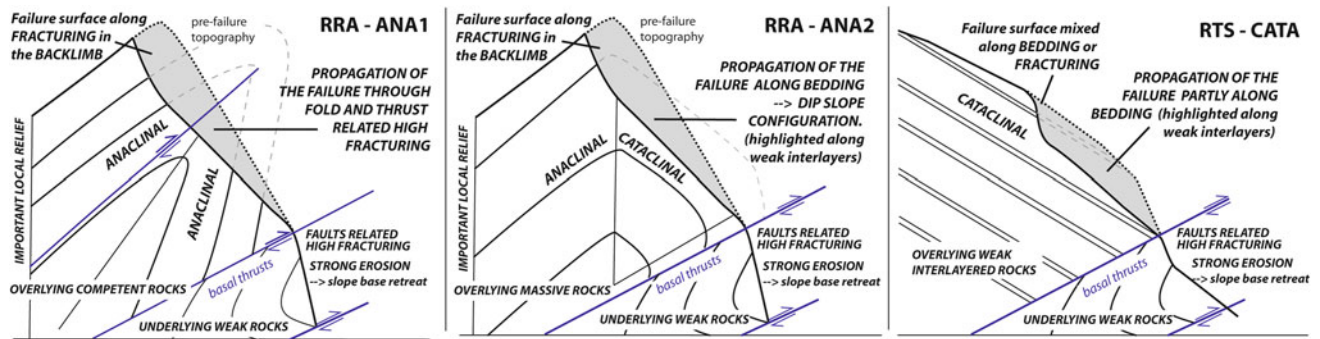


Fig. 99.4 Hypothetic summary sketch of the most frequently observed structural configuration for RSD: ANA1 32 % of RRA with a failure surface propagating through fracturing only in pure anaclinal slope. ANA2 27 % of RRA with initiation of the failure surface in anaclinal

and propagation along bedding in cataclinal slope. CATA 57 % of RTS with initiation of the failure and propagation partly along bedding, partly along fracturing with no simple failure surface

a distance of 200 m. 27 % of the RSD are crossed by a thrust and 51 % are located at a distance of 200 m. A clear link can therefore be expressed between the proximity of these structures and the development of RSD in the LRA (Figs. 99.2b and 99.3e). The distribution of the TOBIA model for the study area (Fig. 99.2c and 99.3f) show a predominance of orthoclinal slopes (39 %) compared to cataclinal (33 %) and anaclinal (28 %) ones. The different slope configurations appear to have a major influence on the RSD categories: RRA are affected at 59 % by anaclinal slopes (respectively 32 % for ANA1 and 27 % for ANA2), RTS are at 57 % in cataclinal slope whereas DSGSD are homogeneously distributed. ANA1 implies that the whole RSD area is affected by anaclinal slope and ANA2 means that the top of the failure surface lies in anaclinal configuration but that the base of the failure surface is affected by cataclinal slope (Fig. 99.4).

99.4 Synthesis and Perspectives

The presence of basal thrusts and folds, their geometry and their lithological properties as well as the local relief appear to be the four main predisposing factors to RSD development in the LRA. The presented inventory led to the identification of 160 events that are mainly spatially distributed within four clusters. Amongst all RSD categories, the control of major tectonic structures is evident especially along major thrusts and anticline hinges where they tend to cluster. This is not surprising as basal thrusts do not only decrease the rock mass strength due to shearing, but also allows competent rock to overlie weak rocks leading to stronger differential erosion of the foot of the slopes (Jackson 2002). If DSGSD appear to be homogeneously distributed, RRA are almost exclusively observed in clusters 1 and 4, whereas RTS are concentrated in clusters 2 and 3. Clusters 1 and 4 are generally associated with higher local relief and

competent lithologies, whereas clusters 2 and 3 are more likely affected by weaker lithologies. This spatial distribution leads to draw a direct relationship between local relief, lithologies and RSD categories distribution. In addition, the orientation of the bedding attitude (TOBIA model) reveals that RTS mainly develop in cataclinal configuration, whereas RRA mostly occur within anaclinal slope. It is interesting to note that this observation differs from the Kanankis country area (few kilometers northward of the present study area) according to Cruden and Eaton (1987) who observed that rockslides are most probable on cataclinal slope.

Based on the preliminary findings of this study, Fig. 99.4 summarizes the three different structural configurations prone to either RRA or RTS depending on (1) presence of anticline hinges/thrust, (2) bedding attitude, (3) lithologies and (4) local relief. Therefore, this study confirms that the same predisposing factors to instabilities proposed for higher relief range are also valid for moderate relief. Further research is however required to interpret the influence of other potential predisposing factors in RSD (glaciation, rainfall, uplift, seismicity...) and to provide more robust statistical analysis.

References

- Agliardi F, Zanchi A, Crosta G (2009) Tectonic vs. gravitational morphostructures in the central Eastern Alps (Italy): constraints on the recent evolution of the mountain range. *Tectonophysics* 474:250–270
- Antinao JL, Gosse J (2009) Large rockslides in the Southern Central Andes of Chile (32–34.5°S): Tectonic control and significance for quaternary landscape evolution. *Geomorphology* 104:117–133
- Besag J (1977) Discussion of Dr Ripley's paper. *J Roy Stat Soc B* 39:193–195
- Clarke BA, Burbank DW (2010) Bedrock fracturing, threshold hillslopes and limits to the magnitude of bedrock landslide. *Earth Planet Sci Lett* 297:577–585

- Cooley MA, Price RA, Dixon JM, Kurtis Kyser T (2011) Along-strike variations and internal details of chevron-style, flexural-slip thrust-propagation folds within the southern Livingstone Range anticlinorium, a paleohydrocarbon reservoir in southern Alberta Foothills, Canada. *AAPG Bulletin* 95(11):1821–1849
- Crosta GB, Frattini P, Agliardi F (2013) Deep-seated gravitational slope deformations in the European Alps. *Tectonophysics* 605:13–33
- Cruden DM, Eaton TM (1987) Reconnaissance of rockslide hazards in Kananaskis Country, Alberta. *Can Geotech J* 24:414–429
- Hermanns RL, Niedermann S, Villanueva Garcia A, Sosa Gomez J, Strecker MR (2001) Neotectonics and catastrophic failure of mountain fronts in the southern intra-Andean Puna Plateau, Argentina. *Geology* 29:619–623
- Hutchinson JN (1988) General report: morphological and geotechnical parameters of landslides in relation to geology and hydrogeology. In: Bonnard C (ed) *Proceedings of the fifth international symposium on landslides*, Balkema, Rotterdam, pp 3–35
- Jackson L (2002) Landslides and landscape evolution in the rocky mountains and adjacent Foothills area, southwestern Alberta, Canada. *Geol Soc Am Rev Eng Geol* 15:325–344
- Kühni A, Pfiffner OA (2001) The relief of the Swiss Alps and adjacent areas and its relation to lithology and structure: topographic analysis from a 250 m DEM. *Geomorphology* 41:285–307
- McMehan ME, Stockmal GS (2013) *Geology, Maycroft, Alberta*, geological survey of Canada, Canadian Geoscience Map 25, scale 1:50000. doi:10.4095/289711
- Meentemeyer RK, Moody A (2000) Automated mapping of alignment between topography and geologic bedding planes. *Comput Geosci* 26:815–829
- Montgomery DR, Brandon MT (2002) Topographic controls on erosion rates in tectonically active mountain ranges, *Earth Plan. Sci Lett* 201:481–489
- Norris DK (1955) Blairmore, Alberta. Canadian Geological Survey, 55–18
- Pedrazzini A, Humair F, Jaboyedoff M, Tonini M (submitted) Characterization and spatial distribution of gravitational slope deformations in the upper Rhone catchment (Western Swiss Alps)
- Ripley BD (1977) Modelling spatial patterns (with discussion). *J Roy Stat Soc B* 39:172–212
- Schmidt KM, Montgomery DR (1995) Limits to relief. *Science* 70:617–620
- Silverman BW (1986) *Density estimation for statistics and data analysis*. Chapman and Hall, New York
- Tonini M, Pedrazzini A, Penna I, Jaboyedoff M (2013) Spatial pattern of landslides in Swiss Rhone Valley, *Natural Hazards*. doi:10.1007/s11069-012-0522-9